Bose-Einstein condensate with higher order interactions: analysis and simulation

Xinran RUAN

Capital Normal University

Joint work with Prof. Weizhu Bao and Prof. Yongyong Cai

Online seminar

Overview

Outline

Bose-Einstein condensate (BEC)

What is Bose-Einstein condensation (BEC)?

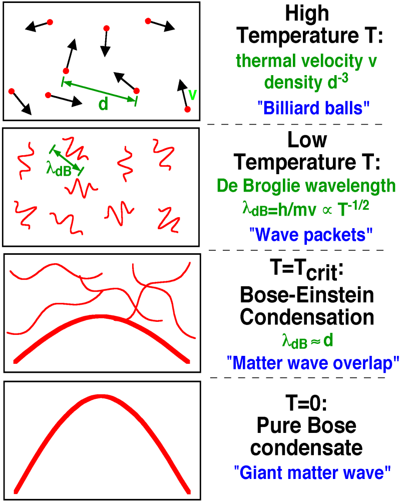

Bose-Einstein condensate (BEC)

What is Bose-Einstein condensation (BEC)?

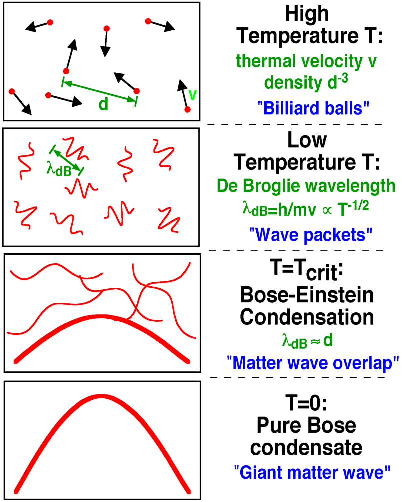

- Predicted by S.N. Bose and A. Einstein in 1924.
- Experimental realization: JILA(1995), NIST, MIT, ...

  – Nobel prize (2001)

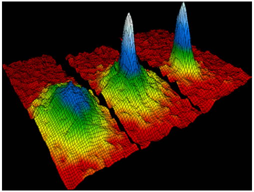

Mathematical modelling

N-body Hamiltonian:

$$H_N = \sum_{j=1}^{N}\left(-\frac{\hbar^2}{2m}\Delta_j + V(\mathbf{x}_j)\right) + \sum_{1\le j<k\le N} V_{\rm int}(\mathbf{x}_j - \mathbf{x}_k).$$

Two key assumptions for mean field model:

- Two-body Fermi contact interaction: $V_{\rm int}(\mathbf{x}_j - \mathbf{x}_k) = g_0\delta(\mathbf{x}_j - \mathbf{x}_k)$.
- Hartree ansatz: $\Psi_N(\mathbf{x}_1,\ldots,\mathbf{x}_N,t) = \prod_{j=1}^{N}\psi(\mathbf{x}_j,t)$.

Mathematical modelling

N-body Hamiltonian:

$$H_N = \sum_{j=1}^{N} \left(-\frac{\hbar^2}{2m}\Delta_j + V(\mathbf{x}_j) \right) + \sum_{1\le j<k\le N} V_{\text{int}}(\mathbf{x}_j - \mathbf{x}_k).$$

Two key assumptions for mean field model:

- Two-body Fermi contact interaction: $V_{\text{int}}(\mathbf{x}_j - \mathbf{x}_k) = g_0\delta(\mathbf{x}_j - \mathbf{x}_k)$.
- Hartree ansatz: $\Psi_N(\mathbf{x}_1, \ldots, \mathbf{x}_N, t) = \prod_{j=1}^{N} \psi(\mathbf{x}_j, t)$.

With the assumptions, we get the Gross-Pitaevskii equation (GPE)

$$i\partial_t\psi(\mathbf{x}, t) = \left[-\frac{1}{2}\Delta + V(\mathbf{x}) + \beta|\psi(\mathbf{x}, t)|^2 \right] \psi(\mathbf{x}, t).$$

Mathematical modelling

N-body Hamiltonian:

$$H_N = \sum_{j=1}^{N} \left(-\frac{\hbar^2}{2m} \Delta_j + V(\mathbf{x}_j) \right) + \sum_{1 \le j < k \le N} V_{\text{int}}(\mathbf{x}_j - \mathbf{x}_k).$$

Two key assumptions for mean field model:

- Two-body Fermi contact interaction: $V_{\text{int}}(\mathbf{x}_j - \mathbf{x}_k) = g_0 \delta(\mathbf{x}_j - \mathbf{x}_k)$.
- Hartree ansatz: $\Psi_N(\mathbf{x}_1, \ldots, \mathbf{x}_N, t) = \prod_{j=1}^{N} \psi(\mathbf{x}_j, t)$.

With the assumptions, we get the Gross-Pitaevskii equation (GPE)

$$i\partial_t \psi(\mathbf{x}, t) = \left[-\frac{1}{2} \Delta + V(\mathbf{x}) + \beta |\psi(\mathbf{x}, t)|^2 \right] \psi(\mathbf{x}, t).$$

Dimension of problem: $3N + 1 \to 3 + 1.$

Higher order correction

- Binary interaction with higher order interaction (HOI) correction

$$V_{\text{int}}(\mathbf{z}) = g_0 \left[\delta(\mathbf{z}) + \frac{g_2}{2} \left(\delta(\mathbf{z}) \Delta_{\mathbf{z}} + \Delta_{\mathbf{z}} \delta(\mathbf{z}) \right) \right], \;\; \mathbf{z} = \mathbf{x}_1 - \mathbf{x}_2.$$

- In certain cases, such as for narrow Feshbach resonances, the higher-order corrections of the binary contact interaction is crucial.

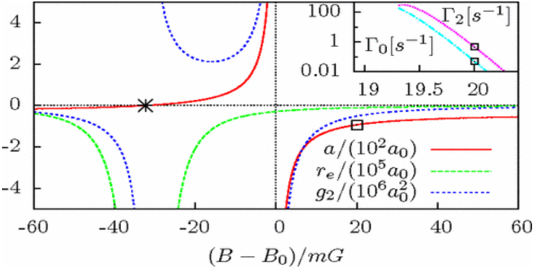

Figure: a_s, r_e and g_2 as a function of B field for the narrow ^{39}K Feshbach resonance. (Phys. Rev. A, 80, 023607)

Modified Gross-Pitaevskii equation

- Modified Gross-Pitaevskii equation (MGPE) in 3D

$$i\partial_t\psi = \left[-\frac{1}{2}\Delta + V(\mathbf{x}) + \beta|\psi|^2 - \delta\Delta|\psi|^2\right]\psi, \quad t \geq 0,\ \mathbf{x} \in \mathbb{R}^3.$$

- Energy

$$E(\psi(\cdot,t)) = \int_{\mathbb{R}^d}\left[\frac{1}{2}|\nabla\psi|^2 + V(\mathbf{x})|\psi|^2 + \frac{\beta}{2}|\psi|^4 + \frac{\delta}{2}|\nabla|\psi|^2|^2\right]d\mathbf{x}.$$

Outline

Dimension reduction problem

- Harmonic potential

$$V(\mathbf{x}) = (\gamma^2 x^2 + \gamma^2 y^2 + \gamma_z^2 z^2)/2.$$

- Key idea

  The motion of a BEC will be frozen in the directions where a sufficiently large trapping frequency is applied.

- Two types
  - Disk-shaped condensate (3D to 2D) : $\gamma_z \gg \gamma$.
  - Cigar-shaped condensate (3D to 1D): $\gamma_z \ll \gamma$.

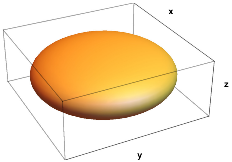

(a) disk-shaped

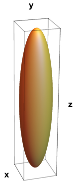

(b) cigar-shaped

Dimension reduction: 3D to 1D

- When $\gamma \gg \gamma_z$, approximate $\psi(\mathbf{x}, t)$ as

$$\psi(\mathbf{x}, t) \approx e^{-i\mu_{2D} t}\chi_{2D}(x, y)\psi_{1D}(z, t),$$

with

$$i\partial_t \psi_{1D}(z, t) = \left[-\frac{1}{2}\partial_{zz} + \frac{\gamma_z^2 z^2}{2} + \beta_1 |\psi_{1D}|^2 - \delta_1(\partial_{zz}|\psi_{1D}|^2)\right]\psi_{1D},$$

where β_1 and δ_1 depending on $\chi_{2D}(x, y)$.

Dimension reduction: 3D to 1D

- When $\gamma \gg \gamma_z$, approximate $\psi(\mathbf{x}, t)$ as

$$\psi(\mathbf{x}, t) \approx e^{-i\mu_{2D} t} \chi_{2D}(x, y) \psi_{1D}(z, t),$$

with

$$i\partial_t \psi_{1D}(z, t) = \left[-\frac{1}{2}\partial_{zz} + \frac{\gamma_z^2 z^2}{2} + \beta_1 |\psi_{1D}|^2 - \delta_1 (\partial_{zz} |\psi_{1D}|^2) \right] \psi_{1D},$$

where β_1 and δ_1 depending on $\chi_{2D}(x, y)$.

Reduce 3D problem to 1D problem.

Question: What is a good approximation of χ_{2D}?

Two possibilities of χ_{2D}

Consider the ground state $\phi_g(x,y,z) = \chi_{2D}(x,y)\phi_{1D}(z)$, then

$$\mu_{2D}\chi_{2D} = \underbrace{-\frac{1}{2}\Delta_{2D}\chi_{2D}}_{\text{(t1)}} + \underbrace{\frac{\gamma^2 r^2}{2}\chi_{2D}}_{\text{(t2)}} + \underbrace{\beta_2|\chi_{2D}|^2\chi_{2D}}_{\text{(t3)}} - \underbrace{\delta_2(\Delta_{2D}|\chi_{2D}|^2)\chi_{2D}}_{\text{(t4)}},$$

where β_2 and δ_2 depends on $\phi_{1D}(z)$.

Two possibilities of χ_{2D}

Consider the ground state $\phi_g(x,y,z) = \chi_{2D}(x,y)\phi_{1D}(z)$, then

$$\mu_{2D}\chi_{2D} = \underbrace{-\frac{1}{2}\Delta_{2D}\chi_{2D}}_{\text{(t1)}} + \underbrace{\frac{\gamma^2 r^2}{2}\chi_{2D}}_{\text{(t2)}} + \underbrace{\beta_2|\chi_{2D}|^2\chi_{2D}}_{\text{(t3)}} - \underbrace{\delta_2(\Delta_{2D}|\chi_{2D}|^2)\chi_{2D}}_{\text{(t4)}},$$

where β_2 and δ_2 depends on $\phi_{1D}(z)$.
Only two possibilities:

- (t1)$\sim$(t2) and (t4) can be neglected – Gaussian approximation.
- (t2)$\sim$(t4) and (t1) can be neglected – Thomas-Fermi approximation.

Two possibilities of χ_{2D}

Consider the ground state $\phi_g(x,y,z) = \chi_{2D}(x,y)\phi_{1D}(z)$, then

$$\mu_{2D}\chi_{2D} = \underbrace{-\frac{1}{2}\Delta_{2D}\chi_{2D}}_{\text{(t1)}} + \underbrace{\frac{\gamma^2 r^2}{2}\chi_{2D}}_{\text{(t2)}} + \underbrace{\beta_2|\chi_{2D}|^2\chi_{2D}}_{\text{(t3)}} - \underbrace{\delta_2(\Delta_{2D}|\chi_{2D}|^2)\chi_{2D}}_{\text{(t4)}},$$

where β_2 and δ_2 depends on $\phi_{1D}(z)$.
Only two possibilities:

- (t1)$\sim$(t2) and (t4) can be neglected – Gaussian approximation.
- (t2)$\sim$(t4) and (t1) can be neglected – Thomas-Fermi approximation.

(t3) always negligible $\Rightarrow$ Always apply Gaussian approximation when $\delta = 0$.

Self consistent iteration

Introduce $\varepsilon = 1/\sqrt{\gamma}$ such that $\varepsilon \to 0^+$, $\tilde{r} = r/\varepsilon^\alpha$ and $\tilde{w}(\tilde{r}) = \varepsilon^\alpha \chi_{_{2D}}(r)$ such that $\tilde{r} \sim O(1)$ and $\|\tilde{w}\| = 1$, then

$$\mu_{_{2D}}\tilde{w} = \underbrace{-\frac{\nabla_\perp^2 \tilde{w}}{2\varepsilon^{2\alpha}}}_{\text{(t1)}} + \underbrace{\frac{\tilde{r}^2\tilde{w}}{2\varepsilon^{4-2\alpha}}}_{\text{(t2)}} + \underbrace{\frac{\beta_2}{\varepsilon^{2\alpha}}\tilde{w}^3}_{\text{(t3)}} - \underbrace{\frac{\delta_2}{\varepsilon^{4\alpha}}\nabla_\perp^2(|\tilde{w}|^2)\tilde{w}}_{\text{(t4)}}.$$

Self consistent iteration

Introduce $\varepsilon = 1/\sqrt{\gamma}$ such that $\varepsilon \to 0^+$, $\tilde{r} = r/\varepsilon^\alpha$ and $\tilde{w}(\tilde{r}) = \varepsilon^\alpha \chi_{_{2D}}(r)$ such that $\tilde{r} \sim O(1)$ and $\|\tilde{w}\| = 1$, then

$$\mu_{_{2D}}\tilde{w} = \underbrace{-\frac{\nabla_\perp^2 \tilde{w}}{2\varepsilon^{2\alpha}}}_{\text{(t1)}} + \underbrace{\frac{\tilde{r}^2\tilde{w}}{2\varepsilon^{4-2\alpha}}}_{\text{(t2)}} + \underbrace{\frac{\beta_2}{\varepsilon^{2\alpha}}\tilde{w}^3}_{\text{(t3)}} - \underbrace{\frac{\delta_2}{\varepsilon^{4\alpha}}\nabla_\perp^2(|\tilde{w}|^2)\tilde{w}}_{\text{(t4)}}.$$

Self consistent iteration (case 1):

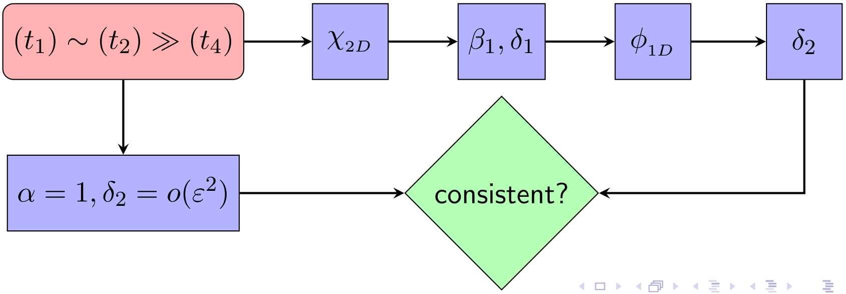

Results for cigar-shaped condensate

TF approximation should be applied to approximate $\chi_{2D}(x, y)$.

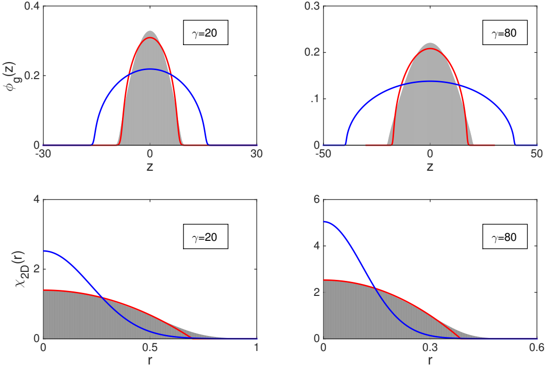

Figure: Red line: TF approximation. Blue line: Gaussian approximation.

Results for disk-shaped condensate

Gaussian approximation should be applied to approximate $\chi_{1D}(z)$.

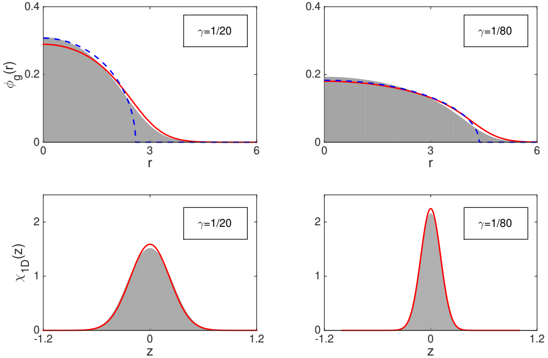

Figure: Red line: Gaussian approximation.

Outline

Ground state

- Minimizer of $E(\cdot)$ under normalization constraint, i.e.

$$\phi_g := \arg\min_{\phi \in S} E(\phi),$$

where

$$E(\phi) = \int_{\mathbb{R}^d} \left[\frac{1}{2}|\nabla \phi|^2 + V(\mathbf{x})|\phi|^2 + \frac{\beta}{2}|\phi|^4 + \frac{\delta}{2}|\nabla|\phi|^2|^2 \right] d\mathbf{x},$$

and $S := \{\phi \mid \|\phi\| = 1,\ E(\phi) < \infty\}.$

Ground state

- Minimizer of $E(\cdot)$ under normalization constraint, i.e.

$$\phi_g := \arg\min_{\phi \in S} E(\phi),$$

where

$$E(\phi) = \int_{\mathbb{R}^d} \left[\frac{1}{2}|\nabla \phi|^2 + V(\mathbf{x})|\phi|^2 + \frac{\beta}{2}|\phi|^4 + \frac{\delta}{2}|\nabla|\phi|^2|^2 \right] d\mathbf{x},$$

and $S := \{\phi \mid \|\phi\| = 1,\ E(\phi) < \infty\}$.

- ϕ_g satisfies the Euler-Lagrange equation

$$\mu_g \phi_g = \left[-\frac{1}{2}\Delta + V(\mathbf{x}) + \beta|\phi_g|^2 - \delta\Delta(|\phi_g|^2) \right] \phi_g.$$

Existence and uniqueness

Theorem (Existence, Uniqueness and Nonexistence)

Suppose $V(\mathbf{x}) \geq 0$ satisfies $\lim_{|\mathbf{x}|\to\infty} V(\mathbf{x}) = +\infty$, then there exists a minimizer $\phi_g \in S$ if one of the following conditions holds

(i) $\delta > 0$ when $d = 1, 2, 3$ for all $\beta \in \mathbb{R}$;

(ii) $\delta = 0$ when $d = 1$ for all $\beta \in \mathbb{R}$, when $d = 3$ for $\beta \geq 0$, and when $d = 2$ for $\beta > -C_b$.

Furthermore, the ground state can be chosen as positive and the positive ground state is unique if $\delta \geq 0$ and $\beta \geq 0$.

In contrast, there exists no ground state if one of the following holds

(i') $\delta < 0$;

(ii') $\delta = 0$ and $\beta < 0$ when $d = 3$; and $\delta = 0$ and $\beta < -C_b$ when $d = 2$.

Proof of existence

Key Point: (Assume $\delta > 0$)

- Show that $E(\cdot)$ is bounded below via the Nash inequality and the Young inequality as follows,

$$\|\rho\|_{L^2}^2 \le C\|\rho\|_{L^1}^{\frac{4}{d+2}}\|\nabla\rho\|_{L^2}^{\frac{2d}{d+2}} \le \frac{\tilde{C}}{\varepsilon} + \varepsilon\|\nabla\rho\|_{L^2}^2, \quad \forall\varepsilon > 0,$$

where $\rho = |\phi|^2$.

Thomas-Fermi (TF) approximation

- Strong interaction: neglect the kinetic energy term.

$$E(\phi) = \int_{\mathbb{R}^d} \Bigg[\underbrace{\frac{1}{2}|\nabla\phi|^2}_{\text{kinetic}} + \overbrace{V(\mathbf{x})|\phi|^2}^{\text{potential}} + \underbrace{\frac{\beta}{2}|\phi|^4 + \frac{\delta}{2}|\nabla|\phi|^2|^2}_{\text{interaction}} \Bigg] \, d\mathbf{x}.$$

Thomas-Fermi (TF) approximation

- Strong interaction: neglect the kinetic energy term.

$$E(\phi) = \int_{\mathbb{R}^d} \Bigg[\underbrace{\cancel{\frac{1}{2}|\nabla\phi|^2}}_{\text{kinetic}} + \overbrace{V(\mathbf{x})|\phi|^2}^{\text{potential}} + \underbrace{\frac{\beta}{2}|\phi|^4 + \frac{\delta}{2}|\nabla|\phi|^2|^2}_{\text{interaction}} \Bigg] d\mathbf{x}.$$

Thomas-Fermi (TF) approximation

- Strong interaction: neglect the kinetic energy term.

$$E(\phi) = \int_{\mathbb{R}^d} \Big[\underbrace{\cancel{\frac{1}{2}|\nabla\phi|^2}}_{\text{kinetic}} + \overbrace{V(\mathbf{x})|\phi|^2}^{\text{potential}} + \underbrace{\frac{\beta}{2}|\phi|^4 + \frac{\delta}{2}|\nabla|\phi|^2|^2}_{\text{interaction}} \Big] \, d\mathbf{x}.$$

Thomas-Fermi (TF) approximation

- Strong interaction: neglect the kinetic energy term.

$$E(\phi) = \int_{\mathbb{R}^d} \Big[\underbrace{\cancel{\frac{1}{2}|\nabla \phi|^2}}_{\text{kinetic}} + \overbrace{V(\mathbf{x})|\phi|^2}^{\text{potential}} + \underbrace{\frac{\beta}{2}|\phi|^4 + \frac{\delta}{2}|\nabla|\phi|^2|^2}_{\text{interaction}} \Big] \, d\mathbf{x}.$$

- For the MGPE: $|\beta| \gg 1$ or $\delta \gg 1$.

Under a harmonic potential

For simplicity, choose $V(\mathbf{x}) = \frac{1}{2}\gamma_0^2\mathbf{x}^2$.

$$\mu\phi = -\frac{1}{2}\Delta\phi + \frac{\gamma_0^2|\mathbf{x}|^2}{2}\phi + \beta|\phi|^2\phi - \delta\Delta(|\phi|^2)\phi \tag{1}$$

$$\Big\Downarrow \tilde{\mathbf{x}} = \mathbf{x}/x_s, \tilde{\phi}(\tilde{\mathbf{x}}) = x_s^{d/2}\phi(\mathbf{x})$$

$$\frac{\mu}{x_s^2}\tilde{\phi} = -\frac{1}{2x_s^4}\Delta_{\tilde{\mathbf{x}}}\tilde{\phi} + \frac{\gamma_0^2|\tilde{\mathbf{x}}|^2}{2}\tilde{\phi} + \frac{\beta}{x_s^{2+d}}\tilde{\phi}^3 - \frac{\delta}{x_s^{4+d}}\Delta_{\tilde{\mathbf{x}}}(|\tilde{\phi}|^2)\tilde{\phi}. \tag{2}$$

- Choose x_s such that $\tilde{x} \sim O(1)$ and $\|\tilde{\phi}\| = 1$.
- Balancing $\frac{\beta}{x_s^{2+d}} \sim \frac{\delta}{x_s^{4+d}} \sim O(1) \Rightarrow$ the borderline $\beta = C_0\delta^{\frac{2+d}{4+d}}$.

Phase diagram

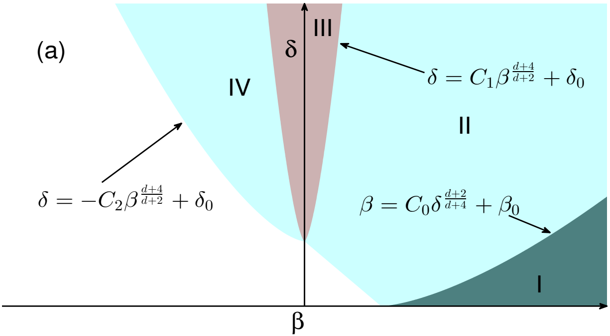

Figure: Phase diagram for extreme regimes under a harmonic potential. In the figure, we choose $\beta_0 \gg 1$ and $\delta_0 \gg 1$, and C_0, C_1 and C_2 positive constants.

Example: TF approximation in regime III

In regime III, i.e. $\beta \ll \delta^{\frac{d+2}{d+4}}$,

$$\mu\phi = -\frac{1}{2}\Delta\phi + \frac{\gamma_0^2|\mathbf{x}|^2}{2}\phi + \beta|\phi|^2\phi - \delta\Delta(|\phi|^2)\phi \tag{3}$$

Example: TF approximation in regime III

In regime III, i.e. $\beta \ll \delta^{\frac{d+2}{d+4}}$,

$$\mu\phi = \cancel{-\frac{1}{2}\Delta\phi} + \frac{\gamma_0^2|\mathbf{x}|^2}{2}\phi + \cancel{\beta|\phi|^2\phi} - \delta\Delta(|\phi|^2)\phi \qquad (3)$$

Example: TF approximation in regime III

In regime III, i.e. $\beta \ll \delta^{\frac{d+2}{d+4}}$,

$$\mu\phi = \cancel{-\frac{1}{2}\Delta\phi} + \frac{\gamma_0^2|\mathbf{x}|^2}{2}\phi + \cancel{\beta|\phi|^2\phi} - \delta\Delta(|\phi|^2)\phi \tag{3}$$

Example: TF approximation in regime III

In regime III, i.e. $\beta \ll \delta^{\frac{d+2}{d+4}}$,

$$\mu\phi = \cancel{-\frac{1}{2}\Delta\phi} + \frac{\gamma_0^2|\mathbf{x}|^2}{2}\phi + \cancel{\beta|\phi|^2\phi} - \delta\Delta(|\phi|^2)\phi \tag{3}$$

The TF density profile:

$$|\phi_{\mathrm{TF}}(\mathbf{x})|^2 = \frac{\gamma_0^2(R^2 - |\mathbf{x}|^2)_+^2}{8(d+2)\delta}, \tag{4}$$

where $R = \left(\frac{(d+2)^2(d+4)\tilde{C}_d}{\gamma_0^2}\right)^{\frac{1}{d+4}} \delta^{\frac{1}{d+4}}$.

Example: TF approximation in regime III

In regime III, i.e. $\beta \ll \delta^{\frac{d+2}{d+4}}$,

$$\mu\phi = \cancel{-\frac{1}{2}\Delta\phi} + \frac{\gamma_0^2|\mathbf{x}|^2}{2}\phi + \cancel{\beta|\phi|^2\phi} - \delta\Delta(|\phi|^2)\phi \tag{3}$$

The TF density profile:

$$|\phi_{\mathrm{TF}}(\mathbf{x})|^2 = \frac{\gamma_0^2(R^2 - |\mathbf{x}|^2)_+^2}{8(d+2)\delta}, \tag{4}$$

where $R = \left(\frac{(d+2)^2(d+4)\tilde{C}_d}{\gamma_0^2}\right)^{\frac{1}{d+4}} \delta^{\frac{1}{d+4}}$.
Set $\rho_g^\varepsilon(\mathbf{x}) = \varepsilon^{-d}|\phi_g(\mathbf{x}/\varepsilon)|^2$ and $\rho_\infty(\mathbf{x}) = \varepsilon^{-d}|\phi_{\mathrm{TF}}(\mathbf{x}/\varepsilon)|^2$ with $\varepsilon = \delta^{-\frac{1}{4+d}}$.

$$\rho_g^\varepsilon(\mathbf{x}) \to \rho_\infty(\mathbf{x}) \text{ in } H^1 \text{ as } \varepsilon \to 0^+ \text{ (i.e. } \delta \to +\infty).$$

Numerical verification

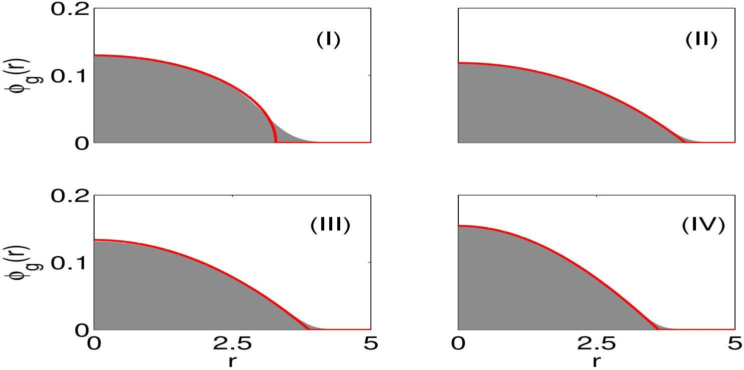

Figure: Red line: TF approximation, and shaded area: numerical solution. ($\gamma = 2$ and (I) $\beta = 1280$, $\delta = 1$; (II) $\beta = 828.7$, $\delta = 1280$; (III) $\beta = 1$, $\delta = 1280$; (IV) $\beta = -828.7$, $\delta = 1280$)

Phase diagram: under a box potential

Box potential:

$$V(\mathbf{x}) = \begin{cases} 0, & \mathbf{x} \in \Omega. \\ \infty, & \mathbf{x} \notin \Omega, \end{cases}$$

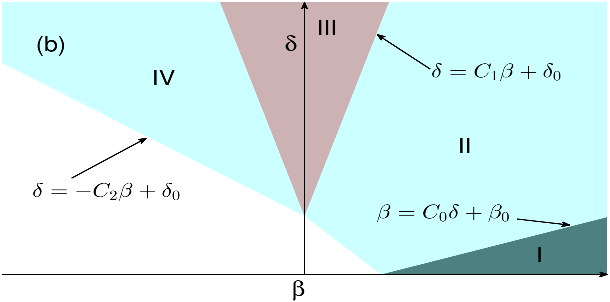

Figure: Phase diagram for extreme regimes under a box potential. In the figure, we choose $\beta_0 \gg 1$ and $\delta_0 \gg 1$, and C_0, C_1 and C_2 positive constants.

Numerical verification

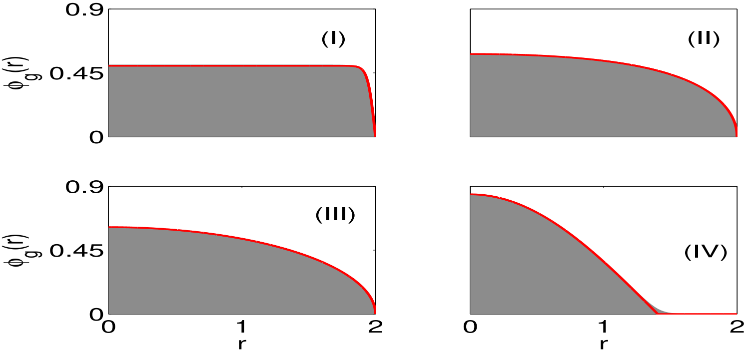

Figure: Red line: analytical TF approximation, and shaded area: numerical solution. ($\Omega = \{\mathbf{x} \,|\, 0 \leq |\mathbf{x}| < 2\}$ and (I) $\beta = 1280$, $\delta = 1$; (II) $\beta = 320$, $\delta = 160$; (III) $\beta = 1$, $\delta = 160$; (IV) $\beta = -400$, $\delta = 80$)

Outline

Method I: normalized gradient flow method

Update from t_n to t_{n+1}:

- Steep descent

$$\phi_t = -\frac{\delta E}{\delta \bar{\phi}} = \frac{1}{2}\Delta\phi - V(\mathbf{x})\phi - \beta|\phi|^2\phi + \delta\Delta(|\phi|^2)\phi.$$

- Projection

$$\phi(\mathbf{x}, t_{n+1}) := \phi(\mathbf{x}, t_{n+1}^{+}) = \frac{\phi(\mathbf{x}, t_{n+1}^{-})}{\|\phi(\mathbf{x}, t_{n+1}^{-})\|}, \quad \mathbf{x} \in \Omega.$$

Method I: normalized gradient flow method

Update from t_n to t_{n+1}:

- Steep descent

$$\phi_t = -\frac{\delta E}{\delta \bar{\phi}} = \frac{1}{2}\Delta\phi - V(\mathbf{x})\phi - \beta|\phi|^2\phi + \delta\Delta(|\phi|^2)\phi.$$

- Projection

$$\phi(\mathbf{x}, t_{n+1}) := \phi(\mathbf{x}, t_{n+1}^{+}) = \frac{\phi(\mathbf{x}, t_{n+1}^{-})}{\|\phi(\mathbf{x}, t_{n+1}^{-})\|}, \quad \mathbf{x} \in \Omega.$$

High restriction on time step, i.e. $\Delta t \lesssim \Delta x^2$, no matter the δ-term is treated semi-implicitly or explicitly.

Convex-concave splitting

- Split the δ-term $E_{\text{HOI}}(\phi) := \frac{\delta}{2}\int_{\mathbb{R}^d} |\nabla|\phi|^2|^2\, d\mathbf{x}$ as

$$E_{\text{HOI}}(\phi) = E_{1,n}(\phi) + E_{2,n}(\phi),$$

  at $t = t_n$, where

$$E_{1,n}(\phi) = 2\delta \int_{\mathbb{R}^d} |\phi|^2(|\nabla\phi|^2 + |\nabla\phi^n|^2)\, d\mathbf{x},$$
$$E_{2,n}(\phi) = -2\delta \int_{\mathbb{R}^d} |\phi|^2|\nabla\phi^n|^2\, d\mathbf{x}.$$

- $E_{1,n}(\phi)$ is convex in ϕ, while $E_{2,n}(\phi)$ is concave.

Normalized gradient flow with convex-concave splitting

- Treating the convex term semi-implicitly and the concave part explicitly,

$$\frac{\tilde{\phi}^{n+1} - \phi^n}{\tau} = \left[\left(\frac{1}{2} + 2\delta\rho^n\right)\Delta - V(\mathbf{x}) - \beta\rho^n\right]\tilde{\phi}^{n+1} + 2\delta|\nabla\phi^n|^2\phi^n,$$

  with $\rho^n = |\phi^n|^2$ and

$$\phi^{n+1} = \frac{\tilde{\phi}^{n+1}}{\|\tilde{\phi}^{n+1}\|}.$$

- Much more stable and unconditionally uniquely solvable for each step.

Numerical results: stability test

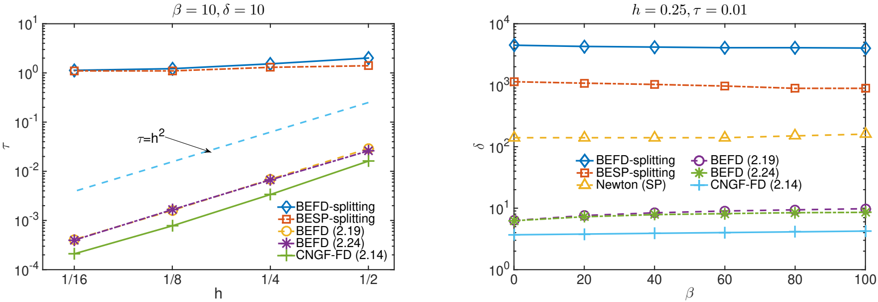

Figure: The lines denote the borderlines of the stability region and the part below the line corresponds to the region where the scheme is stable.

Method II: via regularized density function formulation

Discretize regularized energy $E^\varepsilon(\cdot)$ via the density $\rho(\mathbf{x})$,

$$E^\varepsilon(\rho) = \int_\Omega \left[\frac{1}{2}|\nabla\sqrt{\rho+\varepsilon}|^2 + V(\mathbf{x})\rho + \frac{\beta}{2}\rho^2 + \frac{\delta}{2}|\nabla\rho|^2\right] d\mathbf{x}.$$

Method II: via regularized density function formulation

Discretize regularized energy $E^{\varepsilon}(\cdot)$ via the density $\rho(\mathbf{x})$,

$$E^{\varepsilon}(\rho) = \int_{\Omega} \left[\frac{1}{2} |\nabla \sqrt{\rho + \varepsilon}|^2 + V(\mathbf{x})\rho + \frac{\beta}{2}\rho^2 + \frac{\delta}{2}|\nabla \rho|^2 \right] d\mathbf{x}.$$

- Change the problem to be a convex optimization problem.
- Quadratic interaction energy terms.
- Regularization of the kinetic energy term is necessary.

Method II: via regularized density function formulation

Discretize regularized energy $E^{\varepsilon}(\cdot)$ via the density $\rho(\mathbf{x})$,

$$E^{\varepsilon}(\rho) = \int_{\Omega} \left[\frac{1}{2} |\nabla \sqrt{\rho + \varepsilon}|^2 + V(\mathbf{x})\rho + \frac{\beta}{2}\rho^2 + \frac{\delta}{2}|\nabla \rho|^2 \right] d\mathbf{x}.$$

- Change the problem to be a convex optimization problem.
- Quadratic interaction energy terms.
- Regularization of the kinetic energy term is necessary.

$$\rho_g^{\varepsilon} = \arg\min E^{\varepsilon}(\rho), \text{ subject to } \|\rho\|_1 := \int_{\mathbb{R}^d} \rho(\mathbf{x})\, d\mathbf{x} = 1, \text{ and } \rho \geq 0.$$

- ρ_g^{ε} is solvable for any $\varepsilon > 0$, $\beta \geq 0$ and $\delta \geq 0$.
- Optimize via APG– rDF-APG method.

Convergence analysis

Question: $\rho_g^{h,\varepsilon} \to \rho_g$?

$$
\begin{tikzcd}
\rho_g^{h,\varepsilon} \arrow[r, "\varepsilon \to 0^+"] \arrow[d, "h \to 0^+"'] \arrow[dr, Rightarrow] & \rho_g^h \arrow[d, dashed] \\
\rho_g^{\varepsilon} \arrow[r, "\varepsilon \to 0^+"] & \rho_g
\end{tikzcd}
$$

Convergence results

Theorem 1

When $\delta > 0$, we have $\rho_g^\varepsilon \to \rho_g$ in H^1.

Theorem 2

Fix ε and denote the error to be $e^\varepsilon = \tilde{\rho}_g^\varepsilon - \rho_g^{h,\varepsilon}$. If $\beta > 0$ and $\delta > 0$ and $|\rho_g^\varepsilon|_{h^2}$ is bounded, then we have

$$|e^\varepsilon|_{h^1} := \|\delta_+ e^\varepsilon\|_{l_2} = \mathcal{O}(h), \quad \|e^\varepsilon\|_{l_2} = \mathcal{O}(h^2),$$

where $\tilde{\rho}_g^\varepsilon$ is the interpolation of ρ_g^ε at the grid points.

Theorem 3

When $\beta > 0$ and $\delta > 0$, the ground state ρ_g^h exists uniquely and we have

$$\rho_g^{h,0} := \lim_{\varepsilon \to 0^+} \rho_g^{h,\varepsilon} = \rho_g^h.$$

Convergence analysis

Question: $\rho_g^{h,\varepsilon} \to \rho_g$?

$$
\begin{tikzcd}
\rho_g^{h,\varepsilon} \arrow[r, "\text{Theorem 3}"] \arrow[d, "\text{Theorem 2}"'] \arrow[dr, Rightarrow] & \rho_g^h \arrow[d, dashed] \\
\rho_g^{\varepsilon} \arrow[r, "\text{Theorem 1}"] & \rho_g
\end{tikzcd}
$$

Accuracy test: spatial error

Choose $V(x) = x^2/2$ with $\beta = 10$ and $\delta = 10$.

Error	$h = 1/8$	$h/2$	$h/2^2$	$h/2^3$	$h/2^4$
$\lvert E^\varepsilon(\rho_{g,h}^{\varepsilon,\mathrm{FD}}) - E^\varepsilon(\rho_g^\varepsilon)\rvert$	6.21E-4	1.60E-4	3.97E-5	9.91E-6	2.45E-6
rate	-	1.96	2.01	2.00	2.02
$\lVert\rho_{g,h}^{\varepsilon,\mathrm{FD}} - \rho_g^\varepsilon\rVert_{l_2}$	8.19E-5	2.04E-5	4.88E-6	9.81E-7	2.42E-7
rate	-	2.00	2.06	2.31	2.02
$\lVert\rho_{g,h}^{\varepsilon,\mathrm{FD}} - \rho_g^\varepsilon\rVert_{h_1}$	3.54E-3	1.77E-3	8.85E-4	4.42E-4	2.20E-4
rate	-	1.00	1.00	1.00	1.01
$\lVert\rho_{g,h}^{\varepsilon,\mathrm{FD}} - \rho_g^\varepsilon\rVert_{\infty}$	9.77E-5	3.12E-5	8.17E-6	1.92E-6	4.01E-7
rate	-	1.65	1.94	2.09	2.26

Table: Spatial resolution of the ground state.

Convergence test: $\varepsilon \to 0$

Choose $V(x) = x^2/2$ with $\beta = 10$ and $\delta = 10$.

ε	10^{-1}	10^{-2}	10^{-3}	10^{-4}	10^{-5}	10^{-6}
$\lvert E^\varepsilon(\rho_g^\varepsilon) - E(\rho_g)\rvert$	1.04E0	2.04E-1	2.84E-2	3.70E-3	4.56E-4	5.62E-5
rate	-	0.71	0.86	0.88	0.90	0.92
$\lVert\rho_g^\varepsilon - \rho_g\rVert_2$	1.54E-1	2.45E-2	2.73E-3	2.95E-4	3.08E-5	3.08E-6
rate	-	0.80	0.95	0.97	0.98	1.00
$\lVert\rho_g^\varepsilon - \rho_g\rVert_\infty$	8.64E-2	1.28E-2	1.43E-3	1.54E-4	1.52E-5	1.70E-6
rate	-	0.83	0.95	0.97	1.00	0.95

Table: Convergence test of the ground state densities as $\varepsilon \to 0^+$.

Efficiency test: compare with wave function formulation

	rDF-APG				Regularized Newton method			
$\delta \backslash \beta$	10	10^2	10^3	10^4	10	10^2	10^3	10^4
1	24.11s	10.01s	3.68s	1.81s	1.16s	1.16s	1.61s	75.52s
10	18.34s	12.39s	4.29s	1.67s	4.54s	3.76s	3.47s	3.85s
10^2	10.66s	8.66s	3.78s	1.58s	18.79s	13.42s	9.36s	7.62s
10^3	5.25s	6.29s	3.66s	1.67s	116.65s	79.41s	45.49s	34.03s
10^4	3.31s	3.60s	3.03s	1.66s	224.05s	222.71s	224.89s	144.14s

Table: CPU time through rDF-APG and the regularized Newton method.

Conclusions

Conclusions

- Dimension reduction problem
- Existence and uniqueness of ground states
- Thomas-Fermi approximations of ground states
- Two numerical schemes for computing ground states

Future work

- Effect of the HOI on the rotating BEC ...
- Efficient and stable schemes for the dynamics of MGPE.
- ......